PAPER

Check for updates

Optical properties of selected 4d and 5d transition metal ion-doped glasses

Hongli Wen, [ID] *[a] Bing-Ming Cheng[b] and Peter A. Tanner[c]

Selected 4d and 5d transition metal ion-doped lead borate ($PbO–B_2O_3$) and sodium borosilicate ($SiO_2–Na_2O–B_2O_3$) glasses have been prepared by the melting-quenching technique and their room temperature optical properties were investigated with a view to future co-doping with lanthanide ions. The oxidation states revealed from the diffuse reflectance spectra, absorption spectra, excitation and emission spectra of the glasses are Nb(V), Ta(V), Mo(V, VI), W(VI), Re(IV, VII), Ru(III, IV, VI), Rh(III), and Ir(III). The Ru, Rh, or Ir ion-doped glasses show distinctive strong absorption bands and a red-shifted absorption edge. Charge transfer emission bands are observed for Nb(V), Ta(V), and Mo(VI) at 474 nm, 420 nm and 553 nm, respectively, whereas no visible emission bands can be attributed to Ru, Rh or Ir species. The X-ray absorption spectra of Mo-doped glasses indicate the predominant tetrahedral Mo(VI) moiety. The presence of intense charge transfer absorption and emission bands for some of the transition metal ions provides us with the vision of energy transfer to co-doped lanthanide ions with the application of downshifted emission for a solar cell.

1 Introduction

Compared with bulk crystalline hosts, glasses have the advantages of easy fabrication, low cost, high mechanical strength, and high chemical durability. Therefore, luminescent glass materials play an indispensable role providing a wide spectral range including the ultraviolet, visible, and infrared regions.[1] Emission from glass materials can be achieved by doping lanthanide or transition metal (TM) ions into the glass host. Research has focused upon rare earth ion-doped transparent solid state materials whereas less attention has been paid to TM ion-doped materials, despite their semiconductor nature,[2] optical switching,[3–5] and a broad range of technological applications especially in lasers, phosphors, solar energy converters, plasma display panels and electronic devices.[6,7] Furthermore, since the outer shell *n*d electrons are sensitive to the surrounding ligands, TM ions can be used to probe glass structure.[8]

This work is devoted to the investigation of the UV-Vis-NIR absorption and the luminescence properties of 4d (Nb, Mo, Ru and Rh) and 5d (Ta, W, Re and Ir) TM ion-doped sodium borosilicate glass, as well as the 4d (Mo and Rh) and 5d (W, Re and Ir) ion-doped lead borate glass. We have previously investigated the corresponding properties of 3d TM ion-doped

glasses.[9,10] The aims of these studies are to provide a solid understanding of the redox and spectral behaviours of TM ions in these glasses as a prerequisite to co-doping with lanthanide ions, with applications in down conversion such as for solar energy conversion. The background information of the electronic structures and spectra of the ions investigated are now briefly described.

The closed-shell TM ions Nb^{5+}, Ta^{5+} and W^{6+} in various oxides have metal–oxygen coordinated polyhedral groups contributing to photoluminescence.[11,12] The niobium complex NbO_4^{3-} has been investigated as a possible blue phosphor.[13] Blue-green emission from Nb^{5+} doped glasses excited by an 800 nm femtosecond laser has been ascribed to the charge transfer transition from O^{2-} to Nb^{5+} ions.[14] Rack *et al.*[15] reported that $Ta_2Zn_3O_8$ thin film emitted light at 385 nm under excitation of 236 nm UV radiation, and that 420 nm blue emission could be observed by filtering. Meng *et al.*[1,16] also reported an intense blue emission centred at 420 nm from tantalum doped silicate glass with composition of $(Ta_2O_5)(CaO)_{10}(SiO_2)_{69}(Na_2O)_{20}$ and suggested that it is due to O^{2-} 2p–Ta^{5+} $5d^0$ charge transfer. By contrast to TaO_4^{3-} and TaO_8^{11-} complexes at room temperature, octahedrally-coordinated $(TaO_6)^{7-}$ systems[11] are known as efficient luminescent moieties by this metal-to-ligand transition.

Tungsten has possible oxidation states from +2 to +6,[17] with the two most important oxidation states in glass, W^{5+} and W^{6+}, reported to coexist in tungsten phosphate glasses.[18] Tungsten ions are six fold-coordinated in glasses[19,20] and form distorted WO_6 octahedra in $NaPO_3–BaF_2–WO_3$ glasses at high concentrations. However, Dong *et al.* reported blue emission at 468 nm

[a] Key Laboratory of Clean Chemistry Technology of Guangdong Regular Higher Education Institutions, School of Chemical Engineering and Light Industry, Guangdong University of Technology, Guangzhou 510006, P. R. China. E-mail: hongliwen@gmail.com

[b] National Synchrotron Radiation Research Centre, Hsinchu, Taiwan

[c] Department of Chemistry, Hong Kong Baptist University, Waterloo Road, Kowloon Tong, Hong Kong S.A.R., P. R. China

from tungsten ion-doped Na_2O–CaO–SiO_2 glasses under 800 nm irradiation and they ascribed this emission to the 2p $O^{2-} \rightarrow d^0$ W^{6+} charge transfer transition of WO_4^{2-} tetrahedra.[21]

The electronic configurations of Mo^{6+}, Mo^{5+} and Mo^{4+} are $4d^0$, $4d^1$ and $4d^2$, respectively. The orthorhombic crystal α-MoO_3 consists of edge-sharing distorted MoO_6 octahedra in chains.[22] The octamolybdate unit in $(NH_4)_6Mo_8O_{27} \cdot 4H_2O$ is built up of distorted MoO_6 octahedra sharing edges and corners. Both molar volume and electrical conductivity measurements indicated that Mo^{6+} ions enter $(MoO_3)_x(PbO)_{1-x-y}(B_2O_3)_y$ glasses as network modifiers.[23,24] From electron spin resonance studies, Boudlich et al.[25] concluded that less than 1% of MoO_3 in $(Li_2MoO_4)_{0.1}(P_2O_5)_{0.9-x}(Li_2O)_x$ glasses is present as Mo^{5+}. Reddy et al.[26] reported that molybdenum ions exist mostly in the Mo^{6+} state in the glasses of composition $(MoO_3)_x(PbO)_{20-x}(Sb_2O_3)_{40}(B_2O_3)_{40}$ for $x \leq 0.6$, and occupy network forming positions with $[MoO_4]^{2-}$ structural units, thereby increasing the rigidity of the glass network. However, when MoO_3 is present at higher concentrations, molybdenum ions exist mostly in the Mo^{5+} state and occupy modifying positions. Similarly, for $(MoO_3)_4(PbO)_{30}(B_2O_3)_{66-x}(TiO_2)_x$ glasses there is a change above $x = 0.8$ in the oxidation state of molybdenum to +5.[27] The 500 nm blue emission from $(Mo_2O_5)_{0.5}(Na_2O)_{20}(CaO)_{15}(SiO_2)_{65}$ glass under 800 nm irradiation has been ascribed to O^{2-} 2p $\rightarrow Mo^{6+}$ $4d^0$ charge transfer in $[MoO_4]^{2-}$ tetrahedra.[21]

All the oxidation states of ruthenium (from $4d^0$ Ru^{8+} to $4d^5$ Ru^{3+}) exhibit colour in aqueous solution due to ligand field splitting and/or charge transfer between the central cation and its ligands.[28]

Under strong ligand fields, the $^1A_{1g}$ state of the $4d^6$ ion Rh^{3+} originates from one of the high energy singlet terms of the free ion, ^1I, dropping very rapidly with 10 Dq and crossing the $^5T_{2g}$ state.[29] The octahedrally-coordinated Rh^{3+} ion has a $^1A_{1g}$ (t_{2g}^6) ground state and the excited states are $^{1,3}T_{1g}$ and $^{1,3}T_{2g}$, belonging to the $t_{2g}^5e_g^1$ configuration, with $^3T_{1g}$ as the low-lying excited state. The absorption spectra should therefore consist of two strong bands corresponding to the spin-allowed transitions $^1A_{1g} \rightarrow {}^1T_{1g}$, $^1T_{2g}$ and two weak bands associated with the spin-forbidden transitions $^1A_{1g} \rightarrow {}^3T_{1g}, {}^3T_{2g}$.[30]

Following the experimental descriptions, the subsequent sections describe the absorption, emission and excitation spectra of the TM-doped glasses. In the case of the Mo-doped glasses, X-ray absorption spectra recorded with synchrotron radiation are also reported.

2 Experimental

2.1 Materials and synthesis

The transition metal ion doped sodium borosilicate glass samples had the following nominal compositions (in mol%): $(TM)_{0.5}(SiO_2)_{49.5}(Na_2O)_{25}(B_2O_3)_{25}$, where TM is one of the 4d-transition metal (Nb, Mo, Ru and Rh) ions or the 5d-transition metal (Ta, W, Re and Ir) ions. The doped lead borate glasses had the general formula $(TM)_x(PbO)_{50-x}(B_2O_3)_{50}$ ($x = 0.5$ and 0.01), where TM is Mo, Rh, W, Re and Ir. For comparison, the reference samples with nominal composition (in mol%) of $(SiO_2)_{50}(Na_2O)_{25}(B_2O_3)_{25}$ and $(PbO)_{50}(B_2O_3)_{50}$ were also studied. The above mole compositions refer to the batch composition and small changes caused by vapourisation during melting are neglected. The starting materials were SiO_2 (silica sand 15–20 mesh extra pure, International Laboratory, USA); Na_2CO_3 (99.5%), H_3BO_3 (99.5%), Nb_2O_5 (99.9%), Ta_2O_5 (99.9%), WO_3 (99%), Re_2O_7 (99.9%), PbO (99.9+%), $Na_2WO_4 \cdot 2H_2O$ (all Sigma-Aldrich); $KReO_4$ (99.9%), $RuCl_3 \cdot xH_2O$ (35.1% Ru), $RhCl_3 \cdot xH_2O$ (32.66% Rh), $IrCl_3 \cdot xH_2O$ (57.41% Ir) (all Precious Metals Online, PMO Pty Ltd); MoO_3 (99.5%) (Fluka Chemika); and $(NH_4)_6Mo_7O_{24}$ (99%) (Reidel-de-Haën).

The components were milled, well-mixed together, and melted at 1430 °C for sodium borosilicate glass or at 1000–1200 °C for lead borate glass, in aluminium crucibles under air. Samples were obtained by quenching the melts on a brass plate preheated at 300 °C. The prepared glass samples were transferred immediately to be annealed at 300 °C for 15 h in an ambient air atmosphere.

2.2 Instrumental methods

Room temperature diffuse reflectance spectra (DRS) of the glass samples were recorded between 190–2000 nm at a resolution of 1 nm using a Perkin-Elmer Lambda 750 Spectrometer. The grating change between 860–900 nm produces a spectral artefact. We have observed in previous reports[9,10] that the quality of DRS is similar to that of transmission spectra for glasses. Room temperature excitation and emission spectra were recorded by a Horiba Jobin Yvon Fluorolog spectrophotometer using a xenon lamp as the light source and the signal was detected by a Hamamatsu R636 photomultiplier.

Photoluminescence and X-ray absorption spectra of glasses and reference compounds were measured at 295 K using the beamlines of BL03 (5–35 eV) and BL01C1 (6–33 keV), respectively, at Hsinchu National Synchrotron Radiation Research Centre (NSRRC). The XANES signals at the K-edge were very weak for lead borate glasses with TM ion concentration of 0.5 mol%, so that additional spectra were also recorded for 2 mol% Mo-doped lead borate glass. Comparison of the XANES spectra was performed after background subtraction and normalization.

3 Results and discussion

3.1 Spectral data of undoped base glasses

The spectral data for the undoped glasses have previously been presented[9,10] and explained and the reader is referred to these reports. Basically, the borosilicate glass exhibits intense absorption at 298 nm and a broad emission band centred at 525 nm. The lead borate glass has strong absorption between 237 nm and 349 nm, with a broad emission peak at 470 nm.

3.2 Niobium-doped sodium borosilicate glass

The closed-shell Nb^{5+} ion usually occupies octahedral sites in solids.[11] The niobium-doped sodium borosilicate glass is colourless. The DRS of $(0.5Nb_2O_5)_{0.5}(SiO_2)_{49.5}(Na_2O)_{25}(B_2O_3)_{25}$ is shown as an inset (i) in Fig. 1 in comparison with that of the base glass $(SiO_2)_{50}(Na_2O)_{25}(B_2O_3)_{25}$. The more intense absorption between 270–299 nm is associated with O^{2-}–Nb^{5+}
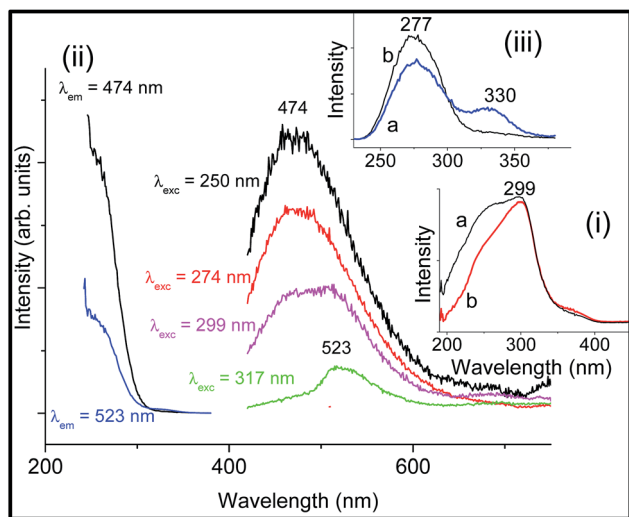
Fig. 1 Room temperature DRS (i), excitation and emission spectra (ii) and excitation spectra (iii) of the Nb-doped glass $(0.5Nb_2O_5)_{0.5}(SiO_2)_{49.5}(Na_2O)_{25}(B_2O_3)_{25}$. In (i), a represents the base glass whereas b shows the Nb-doped glass. The intensities of the spectra in (ii) are not to scale whereas (iii) represents the absolute intensity for the excitation spectra of 523 nm (a) and 474 nm (b) emissions.

Fig. 2 Room temperature excitation and emission spectra of the Ta-doped glass $(0.5Ta_2O_5)_{0.5}(SiO_2)_{49.5}(Na_2O)_{25}(B_2O_3)_{25}$. The peak maxima are marked in nm.

charge transfer. The room temperature excitation and emission spectra of the Nb-doped glass are also shown in Fig. 1(ii). The emission band centred at 523 nm is observed under excitation of 317 (or 330 nm, not shown) with an intensity comparable to that of the undoped sodium borosilicate glass, so that it corresponds to the glass matrix. Two emission bands are observed under excitation of 299 nm. The emission band centred at 474 nm is uniquely observed under excitation of 250 or 274 nm. Zeng et al.[14] have reported that the charge transfer emission band of O^{2-}–Nb^{5+} occurs at 480 nm in $(Nb_2O_5)_1(SiO_2)_{69}(Na_2O)_{20}(CaO)_{10}$ glass under 250 nm and 267 nm excitation, which is therefore similar to our observation. Fig. 1(iii) shows more clearly the absolute intensities in the excitation spectra when monitoring the 523 nm (a) and 474 nm (b) emissions. The maximum of the $O^{2-} \to Nb^{5+}$ charge transfer absorption is observed at 277 nm. No visible emission was observed under excitation by an 800 nm diode laser at 600 mW power.

3.3 Tantalum-doped sodium borosilicate glass

Tantalum produces no colour in sodium borosilicate glass. The room temperature DRS of $(0.5Ta_2O_5)_{0.5}(SiO_2)_{49.5}(Na_2O)_{25}(B_2O_3)_{25}$ glass provides a spectrum completely coincidental with that of undoped sodium borosilicate glass, with a strong UV absorption located at 297 nm. Fig. 2 shows the room temperature excitation and emission spectra of the Ta-doped glass $(0.5Ta_2O_5)_{0.5}(SiO_2)_{49.5}(Na_2O)_{25}(B_2O_3)_{25}$. The emission band centred at 525 nm is observed under excitation of 317 nm, attributed to the host glass emission since the intensity is similar to that of the undoped sodium borosilicate glass. Emission at 420 nm is observed under excitation of 250 nm and is associated with the charge transfer transition of $(TaO_6)^{7-}$.
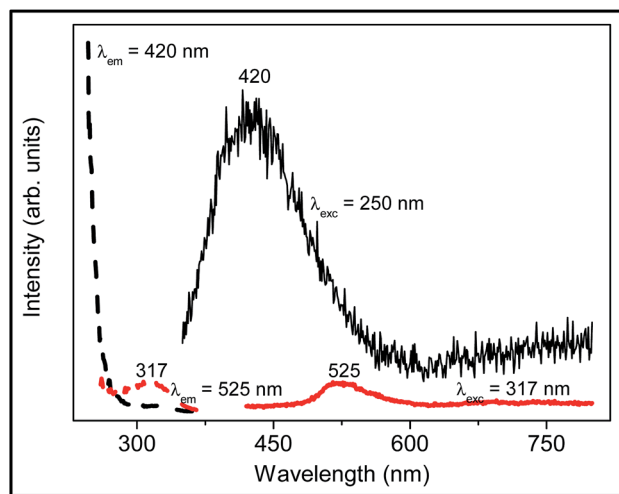
3.4 Molybdenum-doped glasses

Molybdenum produces no colour in sodium borosilicate glass. The obtained Mo-doped lead borate glasses are colourless ($x = 0.01$) and pale yellow ($x = 0.5$) in colour. The Mo K-edge XANES of MoO_3 and $(NH_4)_6Mo_7O_{24}$ doped into lead borate glass, and of MoO_3 doped into sodium borosilicate glass are very similar, Fig. 3(a), and indicate the presence of Mo in the 6 + oxidation state from the pre-edge peak at 20 005 eV. The pre-edge absorption is due to the 1s(Mo) → 4d(Mo) + 2p(O) electronic transition which is dipole forbidden in the case of Mo situated at an inversion centre, but gaining intensity for tetrahedral and distorted octahedral coordination via p–d wavefunction mixing. The large intensity of the pre-edge peak, different from the weak shoulders in the XANES of Mo-doped into phosphate glasses,[31] thus suggests that tetrahedral $[MoO_4]^{2-}$ units are present in the glasses. The EXAFS-k^3 spectra are also very similar for the two glass samples, indicating similar Mo–O bond lengths and plots of Fourier transform magnitude $k^3\chi(k)$ and distance exhibit two major peaks which could indicate distinct Mo–O distances (both spectra not shown) or scattering from another neighbour. Fitting of the Fourier transform spectra gives Mo–O bond distances of 1.774 Å and 1.761 Å for the lead borate glass and borosilicate glass (inset, Fig. 3(a)), respectively, which are shorter than for bridging molybdate groups or hexa-coordinated molybdenum. The Mo–O bond distances in $XMoO_4$ (X = Ca, Sr) are 1.757 ± 0.005 Å and 1.766 ± 0.005 Å, respectively.[32] These conclusions are in agreement with those from the study of Mo doped into nuclear glasses[33] and PbO–Sb_2O_3–B_2O_3 glasses at low Mo concentration[26] but differ from other reports of glasses where the existence of Mo^{5+} has been indicated[34–36] and Mo^{3+} was found.[37] However, firm evidence for the presence of Mo^{5+} species in addition to that of tetrahedral $[MoO_4]^{2-}$ is included below.

Sodium borosilicate glass containing 0.5 mol% MoO_3 reveals a prominent ultraviolet absorption band with the peak at 317 nm, and with no clear absorption bands in the visible
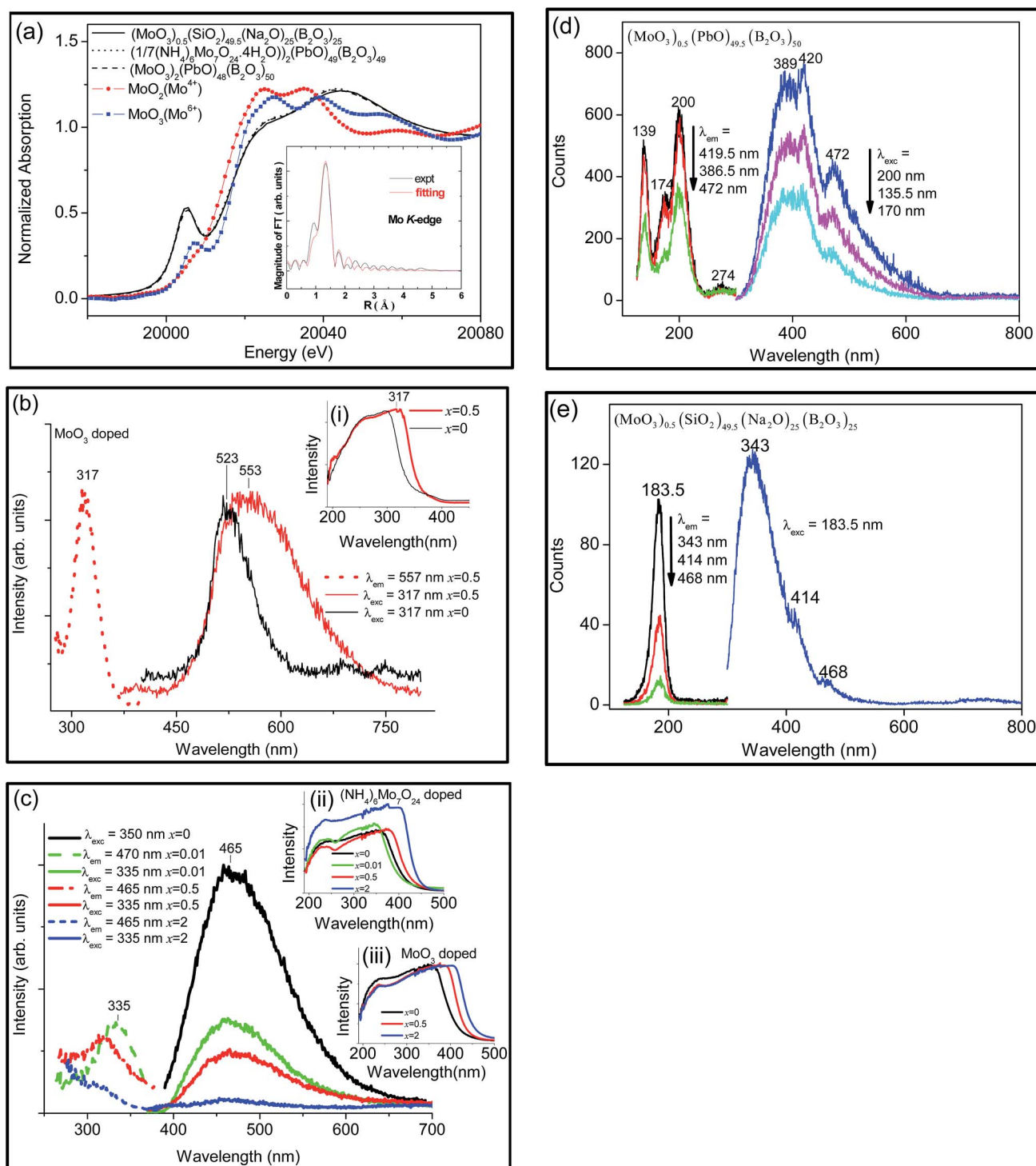
Fig. 3 (a) Normalized Mo K-edge XANES of Mo-doped glasses and comparison with Mo^{4+} and Mo^{6+} species. The inset shows the fitting of the Fourier transform spectrum for $(MoO_3)_{0.5}(SiO_2)_{49.5}(Na_2O)_{25}(B_2O_3)_{25}$; (b) 295 K excitation and emission spectra, and DRS [inset (i)] of $(MoO_3)_x(SiO_2)_{50-x}(Na_2O)_{25}(B_2O_3)_{25}$ x = 0, 0.5; (c) 295 K excitation and emission spectra, and DRS [inset (ii)] of $[1/7(NH_4)_6Mo_7O_{24}\cdot4H_2O]_x(PbO)_{50-x}(B_2O_3)_{25}$ x = 0, 0.01, 0.5, 2, in comparison with DRS [inset (iii)] of $(MoO_3)_x(PbO)_{50-x}(B_2O_3)_{25}$ x = 0, 0.5, 2; 295 K excitation and emission spectra using synchrotron radiation of (d) $(MoO_3)_{0.5}(PbO)_{49.5}(B_2O_3)_{25}$ and (e) $(MoO_3)_{0.5}(SiO_2)_{49.5}(Na_2O)_{25}(B_2O_3)_{25}$. In (b)–(d) and (e) the intensities are arbitrary. Peak wavelengths are marked in nm.

spectral region, Fig. 3(b) inset (i). The slight red-shift of absorption edge from that of the base glass due to the addition of MoO_3 may be ascribed to the charge transfer from O^{2-} to Mo^{6+} ions.[38,39] Lead borate glasses containing Mo in the progressive range from 0.01 mol% to 2 mol% also show a red-shift up to 400 nm, Fig. 3(c) inset (ii)–(iii). The presence of

Mo^{3+} in $(P_2O_5)_{55}(Li_2O)_{30}(CaO)_{10}(Al_2O_3)_{4.8}(MoO_3)_{0.2}$ glasses was made from the observation of a weak emission band at 850 nm (ref. 37) but this band is not observed from our samples, nor the absorption band of Mo^{5+} between 500–950 nm.[40]

Fig. 3(b) shows the broad visible emission band of $(MoO_3)_{0.5}(SiO_2)_{49.5}(Na_2O)_{25}(B_2O_3)_{25}$ under ultraviolet excitation. The emission is assigned to the charge transfer $t_1 \rightarrow 2e$ emission in the region between 500 and 590 nm of $[MoO_4]^{2-}$.[11,41] Blasse[11] reports the absence of emission from $[MoO_6]^{6-}$ compounds.

Fig. 3(c) shows the corresponding emission and excitation spectra for Mo-doped lead borate glasses. The emission spectrum of $PbMoO_4$ is sensitive to the synthesis conditions[42] but the absence of an emission band at ~520 nm shows that the molybdate tetrahedra are not linked to lead ions in the glass.[43] Using excitation wavelengths in the range from 335 nm to 350 nm in Fig. 3(c), the emission arises from the glass matrix and it is quenched for higher molybdenum concentrations.

The Mo-doped lead borate glass was also investigated with synchrotron radiation excitation (Fig. 3(d)). The photoluminescence spectrum does not exhibit change with the different excitation lines and exhibits three peaks at 389, 420 and 472 nm. The excitation spectra of these emissions each display peaks at 139, 174 and 200 nm. The emission bands therefore correspond to the same species. The 183.5 nm-excited spectrum of the borosilicate glass doped with MoO_3, Fig. 3(e), shows three analogous bands to those of the lead borate glass, but shifted and with different relative intensities. The excitation spectra of the emission bands produce only one feature, however, in contrast to Fig. 3(d).

It is clear that Fig. 3(d) and (e) differ considerably from the published absorption spectra of bulk or thin film-MoO_3.[44,45] However, it is noted that the emission spectra in Fig. 3(d) and (e) are similar to the emission spectrum of MoO_3 nanoparticles deposited on thin films using 250 nm excitation, where three major peaks are observed at 343, 411 and 470 nm.[46] The band gaps of the nanoparticles were between 3.2–3.6 eV, compared with that of bulk MoO_3 (2.9 eV). The interpretation of the spectra (and structure) of MoO_3 has not only received different viewpoints, but the spectra themselves differ considerably in literature publications. Blasse reported that bulk Mo^{6+} in tetrahedral α-MoO_3 only shows very weak emission at 295 K, and at 4.2 K the maximum intensity of the broad band is at 750 nm.[47] Otherwise the structure has been described as Mo^{5+} ions in distorted octahedral and other coordination environments, from electron spin resonance measurement.[48] The spectra have been assigned to exciton traps, impurities, charge transfer and/or d-electron transitions. We interpret the spectra as due to the presence of $4d^1$ Mo^{5+} in a distorted octahedral environment arising from loss of oxygen (also found by electron spin resonance measurements[49]). The highest energy emission transition (at 343, 389 nm in Fig. 3(d) and (e), respectively) is then assigned to the maximum of the $^2E \rightarrow {}^2T_2(1)$ transition (where 1 represents the electronic ground state level), whereas the other two bands may correspond to the transitions to the higher-energy crystal field states of $^2T_2$. The value of 10 Dq is then about 23 000–25 000 cm^{-1}. The features in the excitation spectrum may correspond to higher terms of $4d^1$ such as $^2S_{1/2}$ and ^2P_J.

3.5 Tungsten-doped glasses

Tungsten produces no colour in sodium borosilicate glass. The DRS of $(WO_3)_{0.5}(SiO_2)_{49.5}(Na_2O)_{25}(B_2O_3)_{25}$ reveals a strong absorption peak at 300 nm but no visible absorption band. The $(Na_2WO_4 \cdot 2H_2O)_x(PbO)_{50-x}(B_2O_3)_{50}$ glass is colourless when $x = 0.01$ and pale yellow in colour when $x = 0.5$. The DRS of these glasses all exhibit a UV absorption peak between 232–367 nm (inset, Fig. 4). Blue tungsten glass,[18,50] as in $(WO_3)_x(PbO)_{50}(P_2O_5)_{50}$ ($x = 0, 0.01, 0.05, 0.5, 2.5, 5$) contains W^{5+} ions,[51] which have an absorption band at ~780 nm. Our results therefore indicate the existence of mainly W^{6+} in the studied glasses.

The room temperature emission spectrum of $(WO_3)_{0.5}(SiO_2)_{49.5}(Na_2O)_{25}(B_2O_3)_{25}$ exhibits a broader and stronger emission band at 520 nm under excitation at 300 nm, than for the undoped glass. The emission band centred at 465 nm under excitation of 330 nm for the $(Na_2WO_4 \cdot 2H_2O)_x(PbO)_{50-x}(B_2O_3)_{50}$ ($x = 0.01$) glass broadens and moves to lower energy as x increases up to 2 (Fig. 4(a)–(c)). Recently, Dong et al.[21] investigated the blue emission at 468 nm from $(W_2O_5)_{0.5}(Na_2O)_{20}(CaO)_{15}(SiO_2)_{65}$ glass with either the irradiation of an 800 nm femtosecond laser or using 256 nm monochromatic light, and they ascribed this emission to the charge transfer between the O^{2-} and W^{6+} ions in the WO_4^{2-} tetrahedron. Blasse[52] has noted that the emission from isolated tungstate groups is quenched at room temperature, although clusters emit more efficiently, and that any observed emission is related to the presence of defect centres. The weak, broad emission band between 400–700 nm in Fig. 4(c) presumably arises from one of these two reasons but the attribution is unclear.
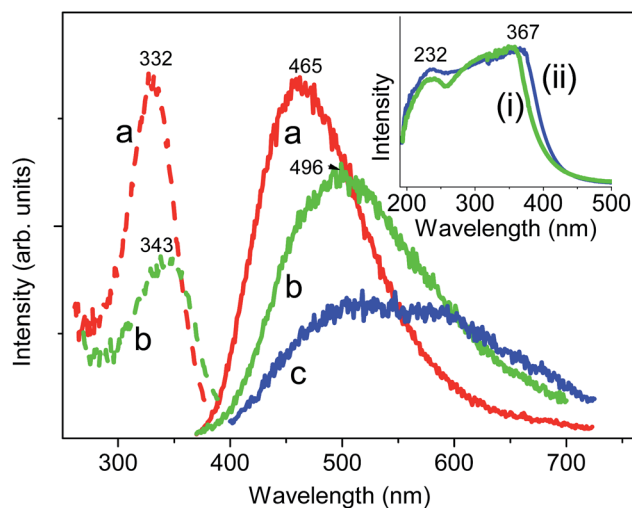

Fig. 4 Room temperature excitation and emission spectra of the tungsten-doped glasses $(Na_2WO_4 \cdot 2H_2O)_x(PbO)_y(B_2O_3)_z$ (not to scale): (a) $x = 0.01, y = 49.99, z = 50$; $\lambda_{exc} = 335$ nm and $\lambda_{em} = 465$ nm; (b) $x = 0.5, y = 49.5, z = 50$; $\lambda_{exc} = 335$ nm and $\lambda_{em} = 488$ nm; (c) $x = 2, y = 49, z = 49$; $\lambda_{exc} = 366$ nm. The inset shows the room temperature DRS of (i) $(Na_2WO_4 \cdot 2H_2O)_{0.5}(PbO)_{49.5}(B_2O_3)_{50}$ and (ii) $(Na_2WO_4 \cdot 2H_2O)_2(PbO)_{49}(B_2O_3)_{49}$.

Abdelghany and co-workers have studied various W-doped glasses with or without the action of ionizing radiation[53–55] and have interpreted the presence of W^{5+} and W^{6+} ions.

From literature data for MWO_4 compounds (M = Mg, Ca, Sr, Ba, Pb) a reasonably linear fit ($R^2_{adj} = 0.9560$, $N = 5$) is obtained for our plot of charge transfer emission band maximum (between 420–470 nm) against cation crystal radius (not shown).

3.6 Rhenium-doped glasses

It was determined from vibrational spectroscopy[56] that rhenium is present in borosilicate glasses as ReO_4^-. Hence due to the absence of d–d transitions, and the high energy of the $O^{2-} \rightarrow Re^{7+}$ charge transfer transition,[57] it was not unexpected that doping Re_2O_7 produces no colour in sodium borosilicate glass. The Re-doped lead borate glass is pale yellow in colour when $x = 0.01$ and 0.5. Re-doped sodium borosilicate glass shows (Fig. 5(a)) an intense UV absorption peak at 303 nm followed by an unresolved weak band at ~455 nm, and a slightly red-shifted absorption edge. The weak feature at 455 nm presumably

corresponds to absorption by a trace of another oxidation state of rhenium. The +6 state exhibits a charge transfer band in this region and the +4 state exhibits the $^2A_2 \rightarrow {}^4T_2$ absorption band. The $x = 0.5$ Re-doped lead borate glass reveals a stronger UV absorption band peaking at 355 nm (Fig. 5(a) inset). The spectra are therefore similar to those of the undoped glasses so that unequivocal assignments of oxidation states other than +7 are not possible from the room temperature absorption spectra.

The excitation and emission spectra of the Re-doped borosilicate glass are shown in Fig. 5(b), with the emission band at 523 nm coming from the glass host. A near infrared band with maximum intensity at 700 nm is also observed under 303 nm and 317 nm excitation which is assigned to the $^2T_2 \rightarrow {}^2A_2$ transition of Re^{4+}.[58]

3.7 Ruthenium-doped sodium borosilicate glass

The Ru-doped sodium borosilicate glass is intense yellow. Black needle-shaped dispersed precipitates were apparent with the addition of 0.5 mol% $RuCl_3$ in sodium borosilicate glass, indicating the excess amount of RuO_2 dispersed in the studied glass, as identified previously.[59,60] The glass reveals a strong UV absorption progressively increasing up to a maximum at 438 nm and a shoulder at ~500 nm, together with a strong absorption peak centred at 711 nm (Fig. 6). The 438 nm band is due to tetrahedrally-coordinated hexavalent ruthenium, Ru^{6+}, and appears at 465 nm in silicate glasses and at 455 nm in phosphate glasses and was assigned to a mixture of ligand and charge transfer band transitions.[28] The shoulder at 500 nm may be due to trivalent ruthenium, Ru^{3+}, assigned to the $^2T_2 \rightarrow {}^2A_2$ transition.[28,61] The absorption band located at 711 nm in Ru-doped sodium borosilicate glass is due to a spin-allowed transition of tetravalent ruthenium, Ru^{4+}.[28,62]

According to Mukerji,[28] the amount of Na_2O in glasses determines the valence states of ruthenium. In silicate glasses with <25 mol% Na_2O, ruthenium is present mainly in octahedral
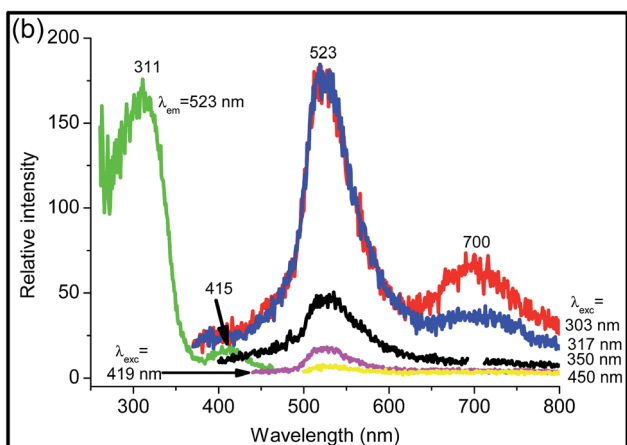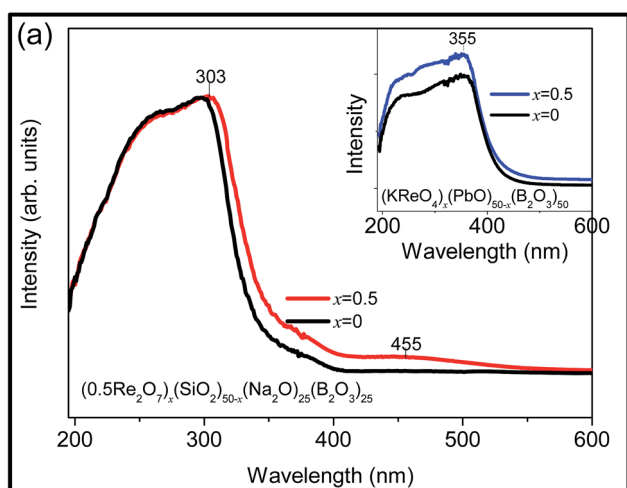

Fig. 5 (a) 295 K DRS of the rhenium-doped glasses $(0.5Re_2O_7)_x(SiO_2)_{50-x}(Na_2O)_{25}(B_2O_3)_{25}$. The inset shows the room temperature DRS of $(KReO_4)_x(PbO)_{50-x}(B_2O_3)_{50}$ for comparison; (b) 295 K emission and excitation spectra of $(0.5Re_2O_7)_{0.5}(SiO_2)_{49.5}(Na_2O)_{25}(B_2O_3)_{25}$.
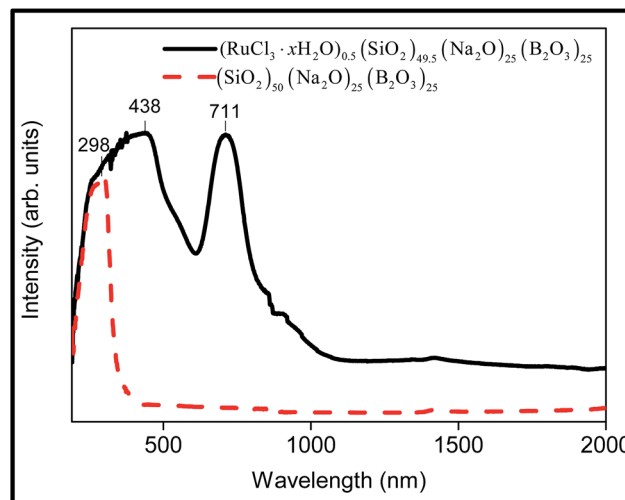

Fig. 6 Room temperature DRS of the Ru-doped glass $(RuCl_3 \cdot xH_2O)_{0.5}(SiO_2)_{49.5}(Na_2O)_{25}(B_2O_3)_{25}$ and comparison with the undoped glass $(SiO_2)_{50}(Na_2O)_{25}(B_2O_3)_{25}$.

coordination since Ru^{4+} and Ru^{3+} are both octahedrally coordinated; silicate glass with >25 mol% Na_2O favours tetrahedrally coordinated ruthenium Ru^{6+}.[28] Thus, in the case of 25 mol% Na_2O in the studied silicate glass, octahedral Ru^{4+} is present together with octahedrally coordinated Ru^{3+}, and tetrahedrally coordinated Ru^{6+}.

3.8 Rhodium-doped glasses

Rh(III) and Ir(III) both belong to the d^6 electron configuration. In octahedral environments, both have a t_{2g}^6 ground state configuration ($^1A_{1g}$), and low-lying states $^3T_{1g,2g}$ and $^1T_{1g,2g}$ of the $t_{2g}^5 e_g^1$ configuration. The Rh-doped sodium borosilicate glass is grey in colour with turbidity. The transparent Rh-doped lead borate glass is yellow and intense yellow in colour when $x = 0.01$ and 0.5, respectively, with small black scattering particles dispersed in the 0.5% Rh doped lead borate glass. Rh-doped sodium borosilicate glass reveals two absorption bands centred at 297 nm and 449 nm, together with progressive medium absorption in the range of 600–2000 nm (Fig. 7, lower). According to the spectral data of other rhodium(III) doped borate and silicate glasses[29] and by using the Tanabe–Sugano diagrams for the d^6 octahedral system,[63] the absorption band at 297 nm can be ascribed to $^1A_1 \rightarrow {}^1T_2$, and at 449 nm to $^1A_1 \rightarrow {}^1T_1$ spin-allowed transitions of rhodium(III) in an octahedral environment.

Rh-doped lead borate glass with $x = 0.01$ reveals a strong UV absorption with maximum at 360 nm, and a shoulder at 440 nm (Fig. 7, upper). Both the borosilicate and lead borate glasses exhibit a very broad absorption from 600–2000 nm for $x = 0.5$. The singlet–triplet transitions $^1A_1 \rightarrow {}^3T_{1,2}$ occur in this wavelength range but the extreme breadth observed in Fig. 7 suggests the presence of charge transfer transitions of Rh and/or metal–metal charge transfer with Pb^{2+}. For example, rhodium and iridium metal oxide nanoparticles deposited on a layered niobate support were found to transfer d-electron density to niobate ions.[64]
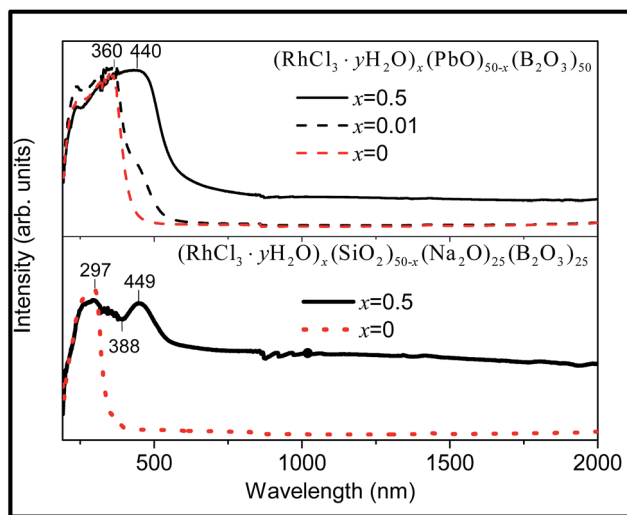

Fig. 7 Room temperature DRS of the Rh-doped glass $(RhCl_3 \cdot yH_2O)_x(SiO_2)_{50-x}(Na_2O)_{25}(B_2O_3)_{25}$ ($x = 0$, 0.5) (lower) and $(RhCl_3 \cdot yH_2O)_x(PbO)_{50-x}(B_2O_3)_{50}$ ($x = 0.5$, 0.01, 0) (upper).
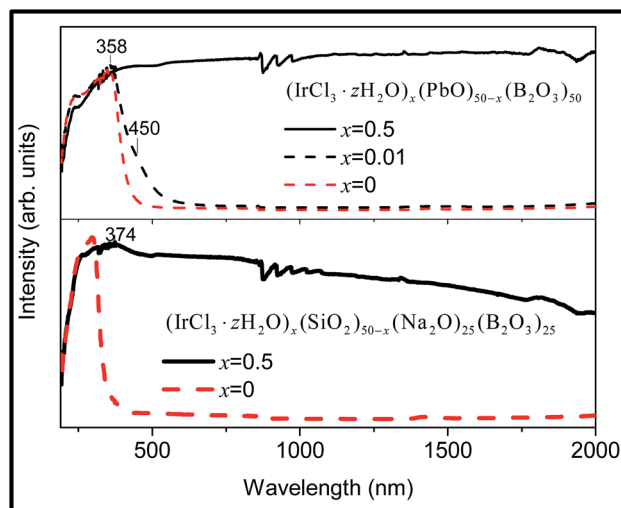
Fig. 8 Room temperature DRS of the Ir-doped glass $(IrCl_3 \cdot zH_2O)_x(SiO_2)_{50-x}(Na_2O)_{25}(B_2O_3)_{25}$ ($x = 0$, 0.5) (lower), and $(IrCl_3 \cdot zH_2O)_x(PbO)_{50-x}(B_2O_3)_{50}$ ($x = 0$, 0.01, 0.5) (upper).

3.9 Iridium-doped glasses

The Ir-doped sodium borosilicate glass is deep grey in colour, revealing a strong UV absorption followed by progressive absorption up to 2000 nm (Fig. 8 lower spectrum). The Ir-doped lead borate glass is yellow and black in colour when $x = 0.01$ and 0.5, respectively. The spectrum of the sample with lower concentration shows a strong UV absorption and a shoulder at 450 nm, with an extension of the absorption to 2000 nm in the sample with higher concentration of Ir (Fig. 8, upper spectrum). The shoulder at 450 nm can be associated with the Ir^{3+} $^1A_1 \rightarrow {}^1T_1$ transition in an oxygen-coordinated octahedral environment and the analogous spin-allowed, spin-forbidden and charge transfer transitions to those of Rh present the continuous absorption in the visible and infrared spectral regions.[65] Ion pair charge transfer has been reported for the Ir–Pb–O system.[66]

4 Conclusions

The study of doped glasses currently attracts attention in solar energy conversion and some new concepts and techniques have recently been suggested.[67–71] The vision of the present study is to utilize intense charge transfer absorption bands of TM ions for solar light absorption with the consequent efficient energy transfer to co-doped lanthanide ions with the downshifted emission at an energy appropriate for a solar cell. Herein, the first step in this direction has required the experimental investigation of TM ion-doped glasses and the interpretation of the spectra obtained. Charge transfer emission bands have been observed for Nb, Ta and Mo-doped glasses. Since these glasses also possess strong charge transfer absorption bands, the energy harvesting and transfer to co-doped lanthanide ions, namely Eu^{3+}, Tb^{3+} and Yb^{3+} appears to be promising.

The major conclusions from this study concern the oxidation states of the species doped into the glasses. The X-ray

absorption near edge spectra of Mo-doped glasses indicate that tetrahedral Mo(VI) exists in the studied lead borate or sodium borosilicate glasses. The oxidation states revealed from the diffuse reflectance spectra, absorption spectra, excitation and emission spectra of the glasses are Nb(V), Ta(V), Mo(V, VI), W(VI), Re(IV,VII), Ru(III, IV, VI), Rh(III), and Ir(III). The Ru, Rh and Ir ion-doped glasses show distinctive strong absorption bands and red-shifted absorption edges.

The use of synchrotron radiation for higher energy excitation of the Mo-doped glass has enabled additional information concerning the presence of oxidation states to be obtained, other than that from XANES and optical spectroscopy.

Acknowledgements

References

1 X. Meng, S. Murai, K. Fujita and K. Tanaka, *Appl. Phys. Lett.*, 2006, **89**, 061914.
2 M. Sayer and A. Mansingh, *Phys. Rev. B: Solid State*, 1972, **6**, 4629.
3 A. Ghosh, *J. Appl. Phys.*, 1988, **64**, 2652.
4 J. Livage, J. P. Jolivet and E. Tronc, *J. Non-Cryst. Solids*, 1990, **121**, 35.
5 Y. Sakurai and J. Yamaki, *J. Electrochem. Soc.*, 1985, **132**, 512.
6 N. J. Kreidl, *J. Non-Cryst. Solids*, 1990, **123**, 377.
7 J. E. Shelby, *Introduction to Glass Science and Technology*, Royal Society of Chemistry, Cambridge, 2nd edn, 2005.
8 J. Wong and C. A. Angell, *Glass: Structure by Spectroscopy*, Marcel Dekker Inc., New York, 1976.
9 H. Wen and P. A. Tanner, *J. Alloys Compd.*, 2015, **625**, 328.
10 H. Wen, P. A. Tanner and B.-M. Cheng, *Mater. Res. Bull.*, 2016, **83**, 400.
11 G. Blasse, The luminescence of closed-shell transition-metal complexes, in *Structure and Bonding*, Springer, Berlin, Heidelberg, 1980, vol. 42, pp. 1–41.
12 Y. Takahashi, K. Kitamura, N. Iyi and S. Inoue, *Appl. Phys. Lett.*, 2006, **88**, 151903.
13 S. H. Shin, D. Y. Jeon and K. S. Suh, *J. Appl. Phys.*, 2001, **90**, 5986.
14 H. Zeng, J. Song, D. Chen, S. Yuan, X. Jiang, Y. Cheng, Y. Yang and G. Chen, *Opt. Express*, 2008, **16**, 6502.
15 P. D. Rack, M. D. Potter, S. Kurinec, W. Park, J. Penczek, B. K. Wagner and C. J. Summers, *J. Appl. Phys.*, 1998, **84**, 4466.
16 X. Meng, K. Tanaka, S. Murai, K. Fujita, K. Miura and K. Hirao, *Opt. Lett.*, 2006, **31**, 2867.
17 J. D. Lee, *A New Concise Inorganic Chemistry*, Van Nostrand Reinhold Co., New York, 3rd edn, 1977.
18 D. Boudlich, L. Bih, M. E. H. Archidi, M. Haddad, A. Yacoubi, A. Nadiri and B. Elouadi, *J. Am. Ceram. Soc.*, 2002, **85**, 623.
19 G. Poirier, F. C. Cassanjes, Y. Messaddeq, S. J. L. Ribeiro, A. Michalowicz and M. Poulain, *J. Non-Cryst. Solids*, 2005, **351**, 3644.
20 G. Poirier, Y. Messaddeq, S. J. L. Ribeiro and M. Poulain, *J. Solid State Chem.*, 2005, **178**, 1533.
21 G. Dong, X. Xiao, B. Qian, J. Song, X. Liu, Q. Zhang, G. Lin, D. Chen and J. Qiu, *J. Optoelectron. Adv. Mater.*, 2009, **11**, 270.
22 H. Negishi, S. Negishi, Y. Kuroiwa, N. Sato and S. Aoyagi, *Phys. Rev. B: Condens. Matter Mater. Phys.*, 2004, **69**, 064111.
23 W. A. Weyl, *Coloured Glasses*, Dawson's of Pall Mall, London, 1959.
24 J. D. Mackenzie, *Modern Aspects of the Vitreous State*, Butterworths, London, 1960.
25 D. Boudlich, M. Haddad, A. Nadiri, R. Berger and J. Kliava, *J. Non-Cryst. Solids*, 1998, **224**, 135.
26 M. S. Reddy, V. L. N. S. Raja and N. Veeraiah, *Eur. Phys. J.: Appl. Phys.*, 2007, **37**, 203.
27 P. S. Prasad, M. S. Reddy, V. R. Kumar and N. Veeraiah, *Philos. Mag.*, 2007, **87**, 5763.
28 J. Mukerji, *Ind. Eng. Chem. Prod. Res. Dev.*, 1972, **11**, 178.
29 A. Paul and J. M. Parker, *Phys. Chem. Glasses*, 1975, **16**, 103.
30 S. C. Weaver and D. S. McClure, *Inorg. Chem.*, 1992, **31**, 2814.
31 A. Kuzmin and J. Purans, *Proc. SPIE*, 1997, **2968**, 180.
32 E. Gürmen, E. Daniels and J. S. King, *J. Chem. Phys.*, 1971, **55**, 1093.
33 G. Calas, M. Le Grand, L. Galoisy and D. Ghaleb, *J. Nucl. Mater.*, 2003, **322**, 15.
34 P. S. Prasad, B. V. Raghavaiah, R. B. Rao, C. Laxmikanth and N. Veeraiah, *Solid State Commun.*, 2004, **132**, 235.
35 S. M. Abo-Naf, *J. Non-Cryst. Solids*, 2012, **358**, 406.
36 O. Cozar, D. A. Magdas and I. Ardelean, *J. Optoelectron. Adv. Mater.*, 2007, **9**, 1730.
37 J. Fernández, A. Mendioroz, R. Balda, M. A. Arriandiaga and M. J. Weber, *Phys. Rev. B: Condens. Matter Mater. Phys.*, 1995, **52**, 181.
38 V. A. Morozov, B. I. Lazoryak, S. Z. Shmurak, A. P. Kiselev, O. I. Lebedev, N. Gauquelin, J. Verbeeck, J. Hadermann and G. Van Tendeloo, *Chem. Mater.*, 2014, **26**, 3238.
39 M. Fournier, C. Louis, M. Che, P. Chaquin and D. Masure, *J. Catal.*, 1989, **119**, 400.
40 M. V. N. P. Rao, L. S. Rao, M. S. Reddy, V. R. Kumar and N. Veeraiah, *Croat. Chem. Acta*, 2009, **82**, 747.
41 Y. Hizhnyi, S. Nedilko, V. Chornii, T. Nikolaenko, I. Zatovsky, K. Terebilenko and R. Boiko, *Solid State Phenom.*, 2013, **200**, 114.
42 M. Tyagi, S. D. G. Desai and S. C. Sabharwal, *J. Lumin.*, 2008, **128**, 22.
43 M. R. D. Bomio, L. S. Cavalcante, M. A. P. Almeida, R. L. Tranquilin, N. C. Batista, P. S. Pizani, M. S. Li, J. Andres and E. Longo, *Polyhedron*, 2013, **50**, 532.
44 P.-R. Huang, Y. He, C. Cao and Z.-H. Lu, *Sci. Rep.*, 2014, **4**, 7131.
45 S. K. Deb and J. A. Chopoorian, *J. Appl. Phys.*, 1966, **37**, 4818.

46 I. Navas, R. Vinodkumar and V. P. M. Pillai, *Appl. Phys. A*, 2011, **103**, 373.

47 G. Blasse and M. Wiegel, *J. Alloys Compd.*, 1995, **224**, 342.

48 S. Morandi, M. C. Paganini, E. Giamello, M. Bini, D. Capsoni, V. Massarotti and G. Ghiotti, *J. Solid State Chem.*, 2009, **182**, 3342.

49 M. Łabanowska, *Phys. Chem. Chem. Phys.*, 1999, **1**, 5385.

50 C. R. Bamford, *Colour Generation and Control in Glass*, Elsevier Scientific Publishing Company, Elsevier North-Holland Inc., Amsterdam, New York, 1977.

51 F. H. ElBatal and S. Y. Marzouk, *J. Mater. Sci.*, 2009, **44**, 3061.

52 G. Blasse and G. J. Dirksen, *J. Solid State Chem.*, 1981, **36**, 124.

53 R. M. M. Morsi, A. M. Abdelghany and M. M. Morsi, *J. Mater. Sci.: Mater. Electron.*, 2015, **26**, 5120.

54 H. A. ElBatal, A. M. Abdelghany, F. H. ElBatal and F. M. EzzElDin, *Mater. Chem. Phys.*, 2012, **134**, 542.

55 A. M. Abdelghany and A. H. Hammad, *J. Mol. Struct.*, 2015, **1081**, 342.

56 P. L. Gassman, J. S. McCloy, C. Z. Soderquist and M. J. Schweiger, *J. Raman Spectrosc.*, 2014, **45**, 139.

57 J. F. H. Custers, *Physica*, 1937, **4**, 426.

58 J. F. Suyver, A. Aebischer, D. Biner, P. Gerner, J. Grimm, S. Heer, K. W. Krämer, C. Reinhard and H. U. Güdel, *Opt. Mater.*, 2005, **27**, 1111.

59 S. R. Butler and J. L. Gillson, *Mater. Res. Bull.*, 1971, **6**, 81.

60 M. Yamashita, H. Yamanaka and K. Sasage, *J. Am. Ceram. Soc.*, 2004, **87**, 967.

61 C. J. Ballhausen, *Introduction to Ligand Field Theory*, McGraw-Hill, New York, 1962.

62 J. Mukerji and S. R. Biswas, *Indian J. Chem.*, 1969, **7**, 1239.

63 Y. Tanabe and S. Sugano, *J. Phys. Soc. Jpn.*, 1954, **9**, 753.

64 M. E. Strayer, T. P. Senftle, J. P. Winterstein, N. M. Vargas-Barbosa, R. Sharma, R. M. Rioux, M. J. Janik and T. E. Mallouk, *J. Am. Chem. Soc.*, 2015, **137**, 16216.

65 B. Gilliams, L. Heerman and C. Görller-Walrand, *J. Alloys Compd.*, 1997, **259**, 153.

66 C. Mullens, M. Pikulski, S. Agachan and W. Gorski, *J. Am. Chem. Soc.*, 2003, **125**, 13602.

67 X. Huang, *J. Alloys Compd.*, 2017, **690**, 356.

68 P. Song, C. M. Zhang and P. F. Zhu, *Ceram. Int.*, 2016, **42**, 11417.

69 S. F. H. Correia, P. P. Lima, E. Pecoraro, S. J. L. Ribeiro, P. S. André, R. A. S. Ferreira and L. D. Carlos, *Prog. Photovoltaics*, 2016, **24**, 1178.

70 G. Lia, C. Zhang, P. Song, P. Zhu, K. Zhu and J. He, *J. Alloys Compd.*, 2016, **662**, 89.

71 J. A. Jiménez and M. Sendova, *Mater. Chem. Phys.*, 2015, **162**, 425.